

Supporting Information

A new general approach to synthesizing filled and yolk-shell structured metal oxide microspheres by applying a carbonaceous template

Young Jun Hong,^a Kwang Chul Roh,^b Jung-Kul Lee*^c and Yun Chan Kang*^a

^aDepartment of Materials Science and Engineering, Korea University, Anam-Dong, Seongbuk-Gu, Seoul 136-713, Republic of Korea. E-mail: yckang@korea.ac.kr

^bEnergy and Environmental Division Korea Institute of Ceramic Engineering and Technology (KICET) Jinju, Gyeongnam 52851, Republic of Korea.

^cDepartment of Chemical Engineering Konkuk University Hwayang-dong, Gwangjin-gu Seoul 143-701, Republic of Korea. E-mail: jkrhee@konkuk.ac.kr

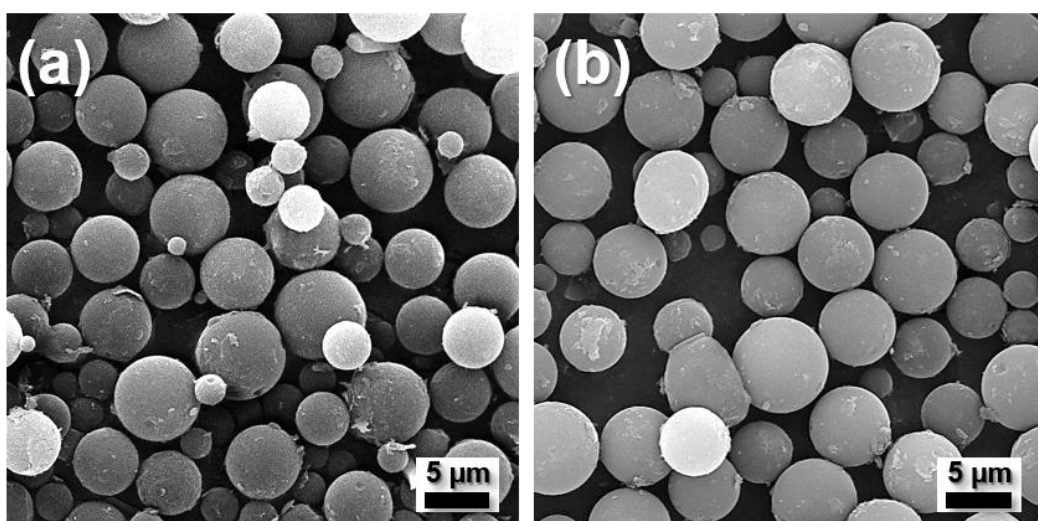


Fig. S1 SEM images of the carbonaceous template microspheres (a) before and (b) after impregnation of $\text{Sn}(\text{Oct})_2$ at the loading rate of 0.3 mL.

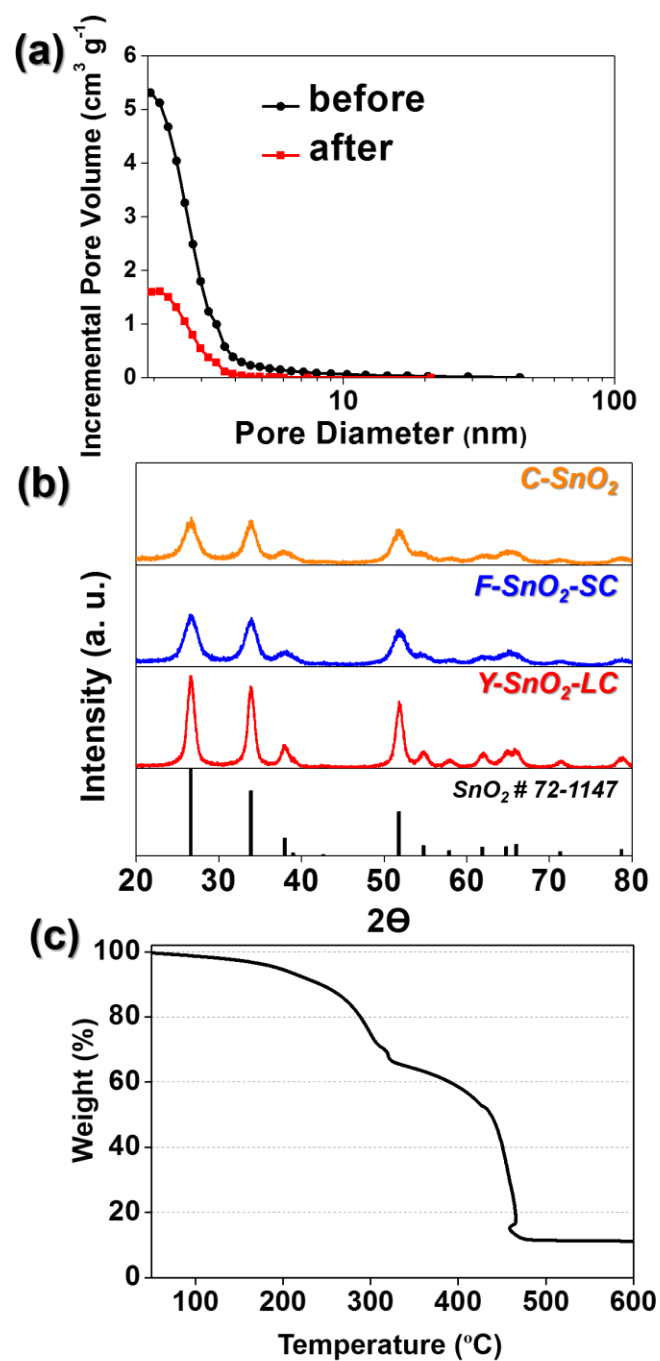


Fig. S2 (a) BJH pore size distributions of the carbon template microspheres before and after Sn(Oct)₂ impregnation, (b) XRD patterns of the C-SnO₂ and filled and yolk-shell structured SnO₂ microspheres, and (c) TG curve of the C-Sn(Oct)₂ composite microspheres measured under air atmospheres.

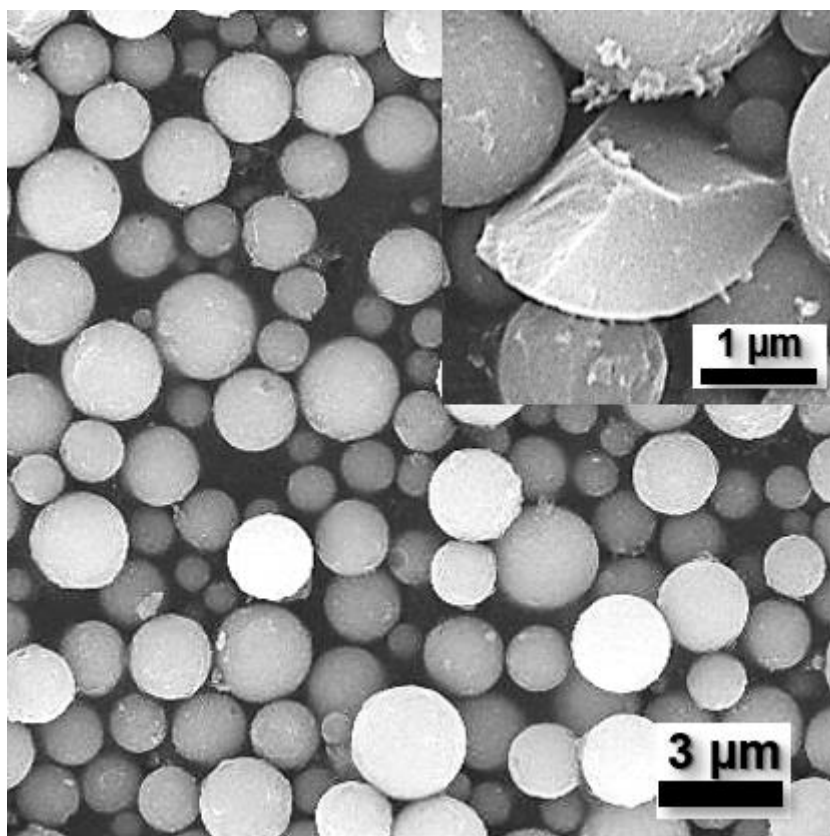


Fig. S3 Morphologies of the SnO₂ microspheres obtained by post-treatment of the C-SnO₂ microsphere (shown in Fig. 1) in an atmosphere with high oxygen concentration and ramping rate of 10 °C min⁻¹ s.

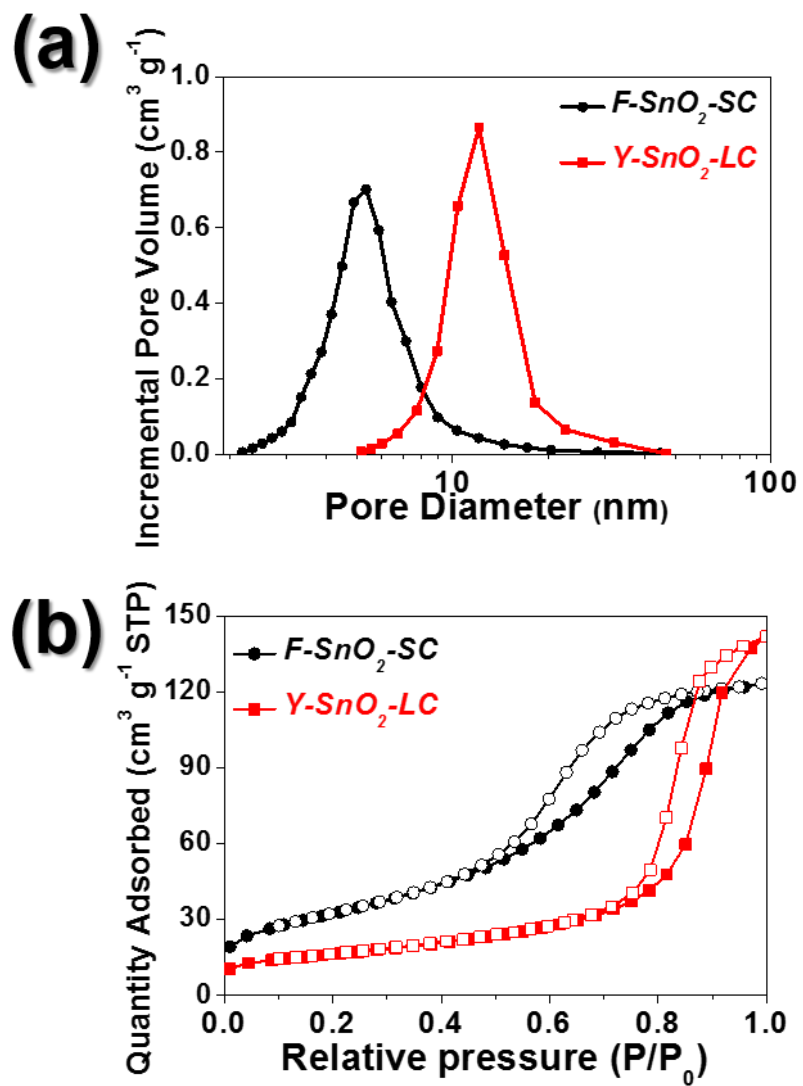


Fig. S4 (a) BJH pore size distributions and (b) N₂ adsorption and desorption isotherms of the yolk-shell and filled structured SnO₂ microspheres.

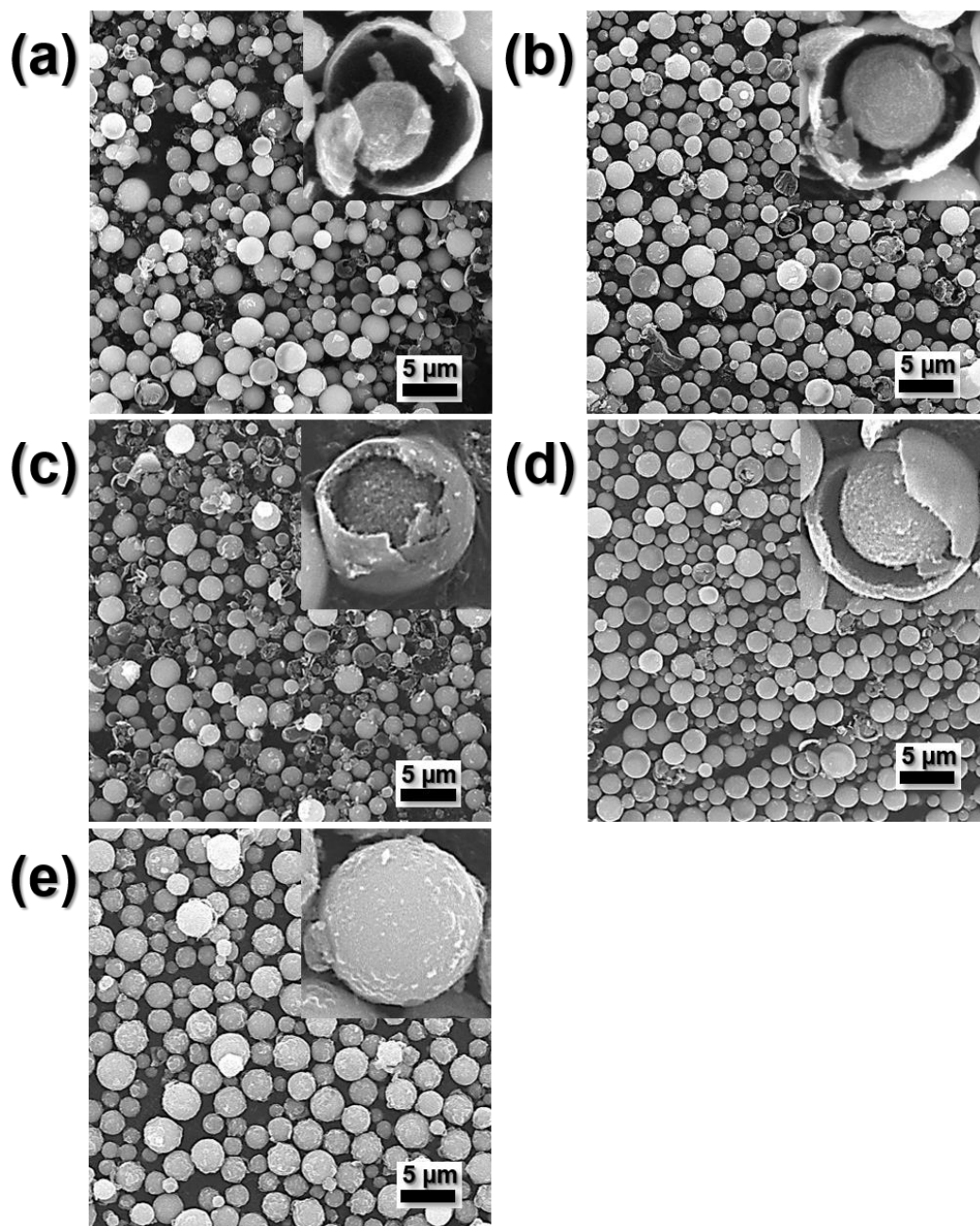


Fig. S5 Morphologies of the SnO₂ microspheres prepared from the carbonaceous template microspheres with various loading rate of tin(II) octoate by post-treatment at 500 °C in an atmosphere with high oxygen concentration and ramping rate of 10 °C min⁻¹: (a) 0.2 ml, (b) 0.4 ml, (c) 0.6 ml, (d) 1.0 ml, and (e) 1.5 ml.

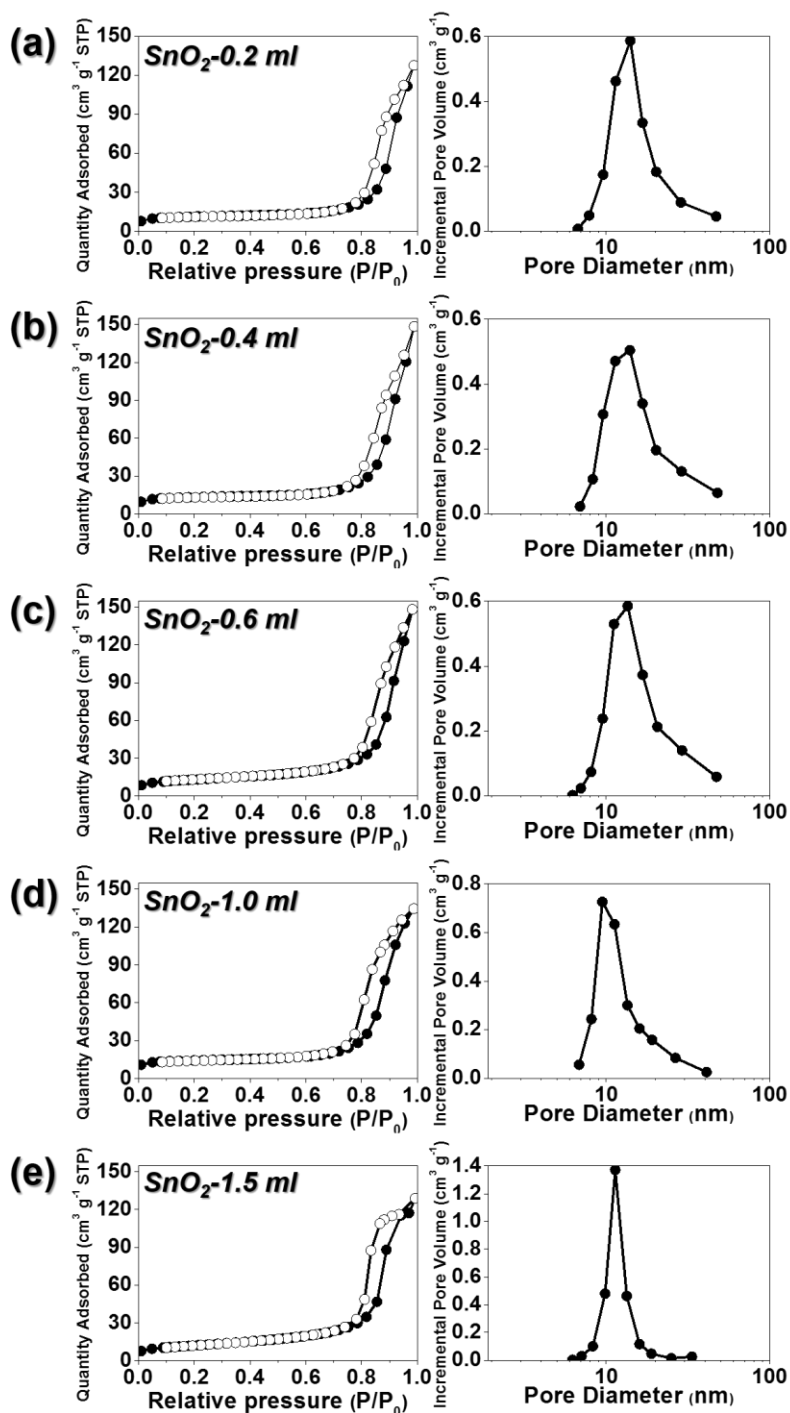


Fig. S6 Nitrogen adsorption and desorption isotherms and BJH pore size distributions of the SnO_2 microspheres formed from the carbonaceous template microspheres with various loading rate of tin(II) octoate by post-treatment at 500°C in an atmosphere with high oxygen concentration and ramping rate of $10^\circ\text{C min}^{-1}$: (a) 0.2 ml, (b) 0.4 ml, (c) 0.6 ml, (d) 1.0 ml, and (e) 1.5 ml.

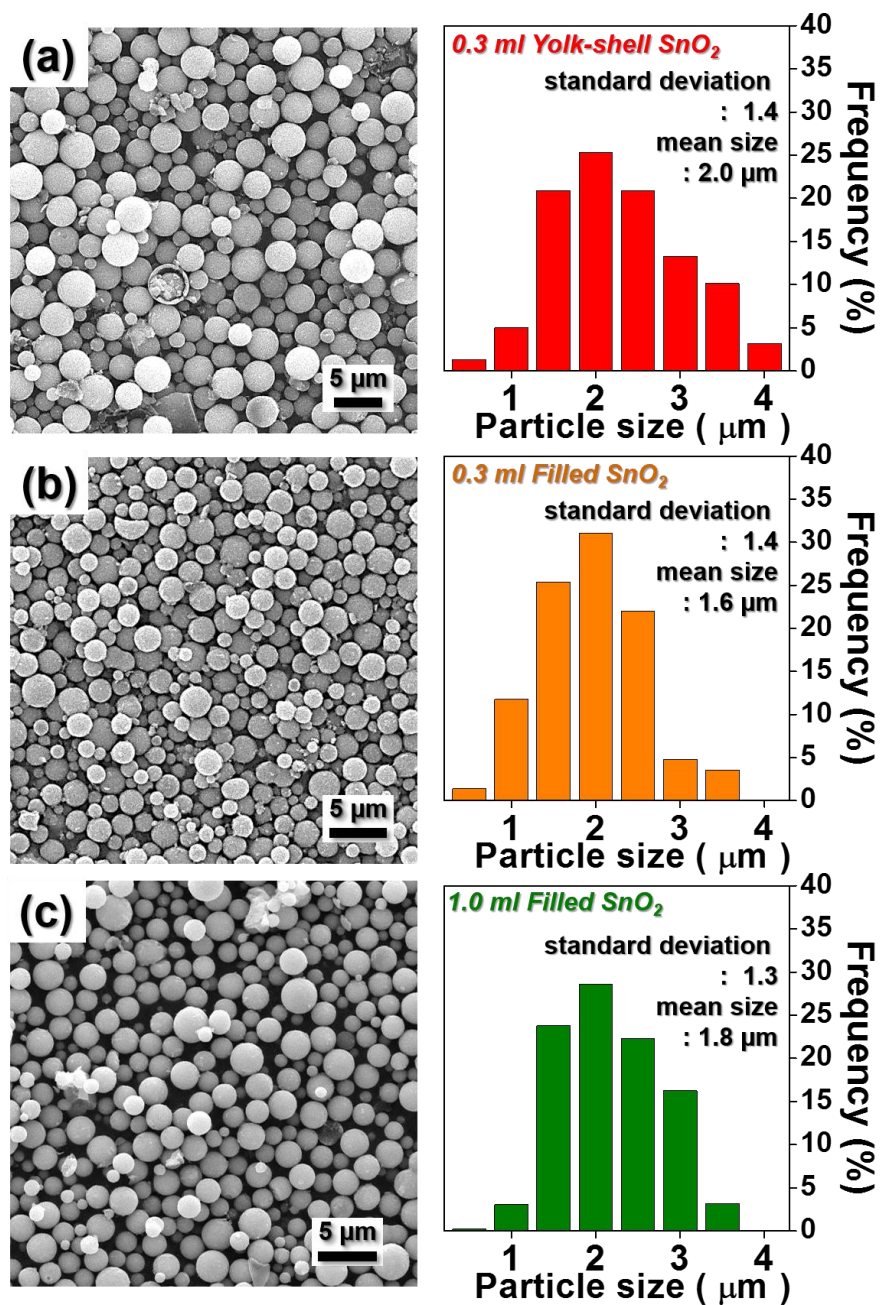


Fig. S7 Morphologies and size distributions of the (a) filled and (b) yolk-shell structured SnO_2 microspheres formed from the $\text{C-Sn}(\text{Oct})_2$ microspheres with the loading rate of 0.3 mL, and (c) filled structured SnO_2 microspheres formed from the $\text{C-Sn}(\text{Oct})_2$ microspheres with loading rate of 1.0 mL.

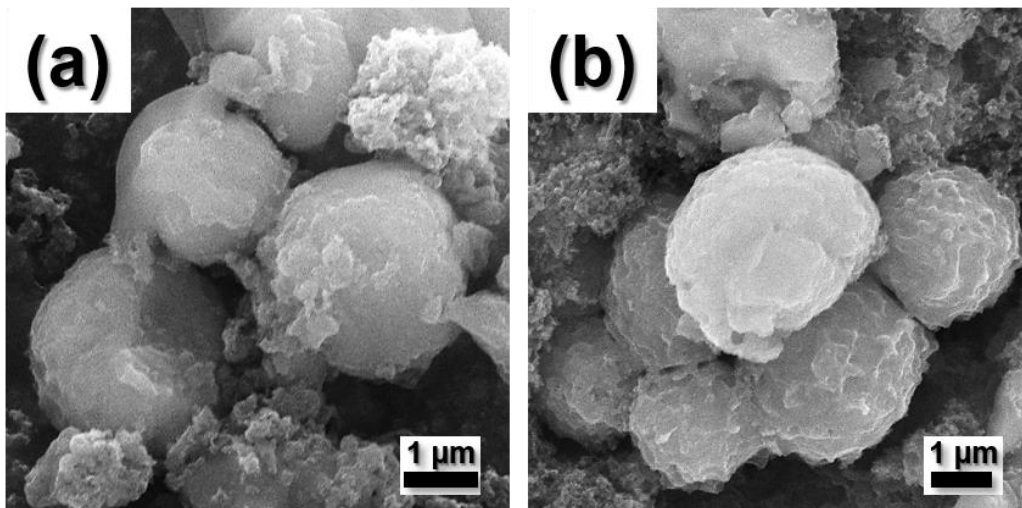


Fig. S8 SEM images of the (a) Y-SnO₂-LC and (b) F-SnO₂-SC microspheres after 100 cycles.

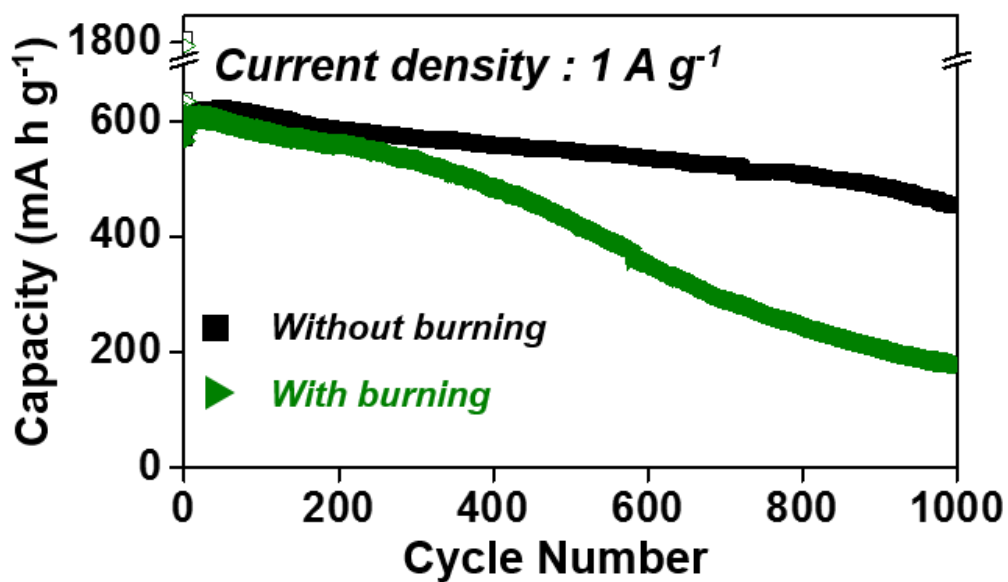


Fig. S9 Cycling performances of the filled structured SnO₂ microspheres prepared by decomposition of the carbonaceous template with and without burning at a constant current density of 1 A g⁻¹.

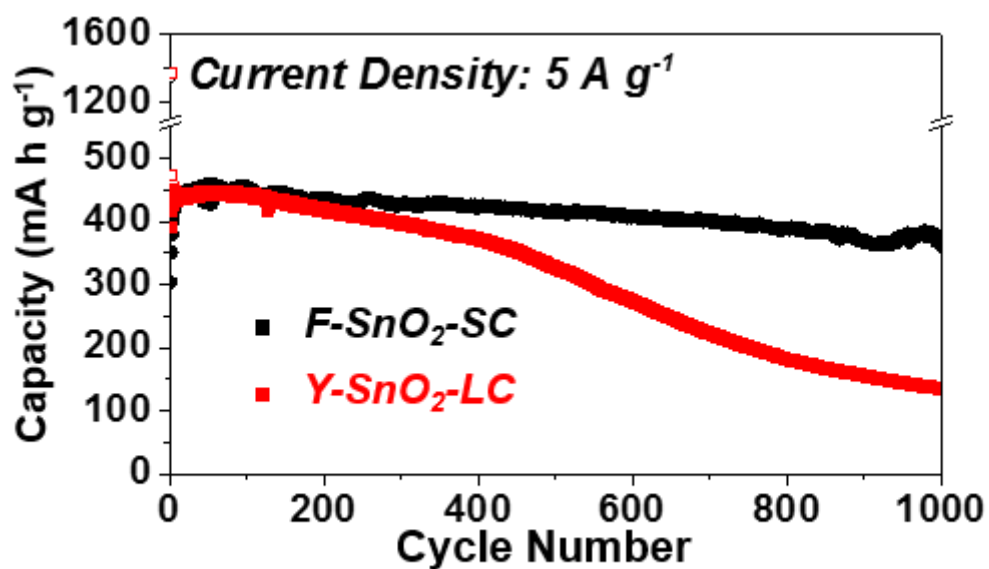


Fig. S10 Cycling performances of the filled and yolk-shell structured SnO₂ microspheres formed from the C-Sn(Oct)₂ microspheres with the same loading rate of 0.3 mL at a constant current density of 5 A g⁻¹.

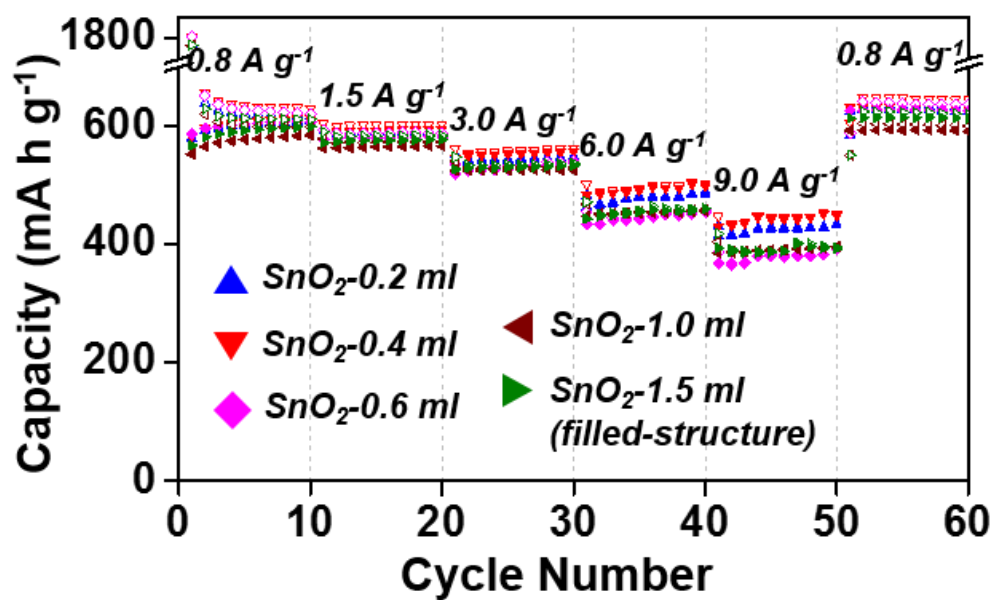


Fig. S11 Rate performances of the SnO₂ microspheres prepared from the carbonaceous template microspheres with various loading rate of tin(II) octoate by post-treatment at 500 °C in an atmosphere with high oxygen concentration and ramping rate of 10 °C min⁻¹.

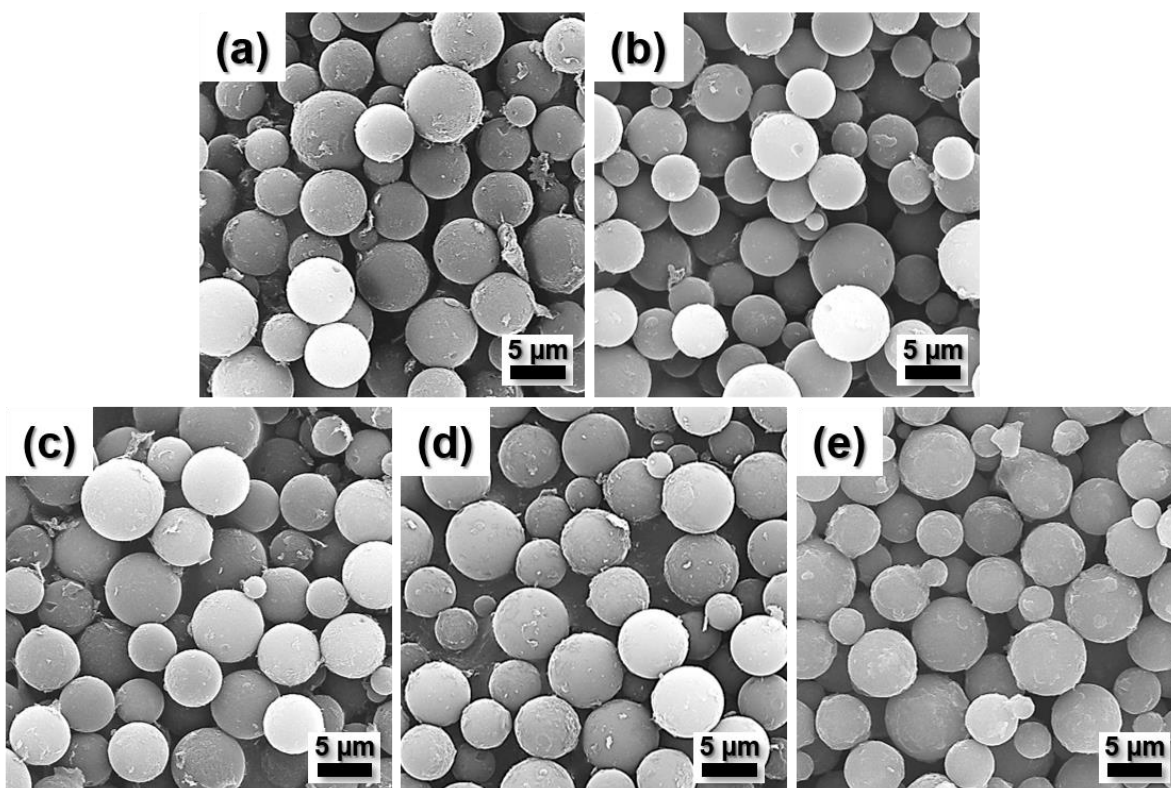


Fig. S12 Morphologies of the carbonaceous template microspheres with various loading rate of tin(II) octoate: (a) 0.2 ml, (b) 0.4 ml, (c) 0.6 ml, (d) 1.0 ml, and (e) 1.5 ml.

Table S1. Cycling and rate performances of various nanostructured SnO₂ materials in lithium-ion batteries.

Various hollow SnO ₂ materials	cycling performance	rate performance	Ref
SnO₂@carbon hollow spheres	Discharge capacity of 643 mA h g ⁻¹ after 300 cycles (at 0.5 A g ⁻¹ , 0–3.0 V)	The discharge capacities were 520 and 210 mA h g ⁻¹ at current densities of 0.2 and 3.0 A g ⁻¹ , respectively. (0–3.0 V)	[57]
SnO₂ hollow spheres	Discharge capacity of 643 mA h g ⁻¹ after 300 cycles (at 2.0 A g ⁻¹ , 0.001–1.0 V)	The discharge capacities were 780 and 597 mA h g ⁻¹ at current densities of 0.5 and 7.0 A g ⁻¹ , respectively. (0.001–1.0 V)	[58]
SnO₂ fiber-in-tube	Discharge capacity of 640 mA h g ⁻¹ after 300 cycles (at 1.0 A g ⁻¹ , 0.001–1.0 V)	The discharge capacities were 774 and 591 mA h g ⁻¹ at current densities of 0.5 and 5.0 A g ⁻¹ , respectively. (0.001–1.0 V)	[59]
Three-dimensional SnO₂@TiO₂ double-shell nanotubes on carbon cloth	Discharge capacity of 400 mA h g ⁻¹ after 100 cycles (at 1.0 A g ⁻¹ , 0.01–3.0 V)	The discharge capacities were 843 and 135 mA h g ⁻¹ at current densities of 0.16 and 7.8 A g ⁻¹ , respectively. (0.01–3.0 V)	[60]
SnO₂/C microspheres	The discharge capacity 50 and 379 mA h g ⁻¹ after 800 cycles. (at 0.1 A g ⁻¹ , 0–3.0 V)	The discharge capacities were 378 and 230 mA h g ⁻¹ at current densities of 0.1 and 0.6 A g ⁻¹ , respectively. (0 – 3.0 V)	[61]
pillar arrays of C-coated hollow SnO₂	Discharge capacity of 488 mA h g ⁻¹ after 50 cycles (at 1.0 A g ⁻¹ , 0.005–2.0 V)	The discharge capacities were 634 and 408 mA h g ⁻¹ at current densities of 0.78 and 7.8 A g ⁻¹ , respectively. (0.005 – 2.0 V)	[62]
Carbon nanotube @SnO₂-Au coaxial nanocable	Discharge capacity of 626 mA h g ⁻¹ after 40cycles (at 0.18 A g ⁻¹ , 0.05–1.2 V)	The discharge capacities were 660 and 392 mA h g ⁻¹ at current densities of 0.18 and 7.2 A g ⁻¹ , respectively. (0.05 – 1.2 V)	[63]

SnO₂-C hollow nanostructures

Discharge capacity of 577 mA h g⁻¹ after 500 cycles (at 0.2 A g⁻¹, 0-3.0 V)

The discharge capacities were 701 and 412 mA h g⁻¹ at current densities of 0.4 and 5.0 A g⁻¹, respectively. (0 – 3.0 V)

[64]

Filled structured SnO₂ microspheres

Discharge capacity of 450 mA h g⁻¹ after 1000 cycles (at 1 A g⁻¹, 1.0 V)

The discharge capacities were 637 and 372 mA h g⁻¹ at current densities of **0.8 and 9.0 A g⁻¹**, respectively. (0.01 – 1.0 V)

This study
